CHEMISTRY OF MATERIALS

ARTICLE

pubs.acs.org/cm

High-Surface-Area SBA-15 with Enhanced Mesopore Connectivity by the Addition of Poly(vinyl alcohol)

Junjiang Zhu,*,† Kamalakannan Kailasam,† Xiao Xie,‡ Reinhard Schomaecker,‡ and Arne Thomas*,†

†Institut für Chemie, Sekr. TC 2, Technische Universität Berlin, Englische Strasse 20, 10587 Berlin, Germany

‡Institut für Chemie, Sekr. TC 8, Technische Universität Berlin, Strasse des 17 Juni 124, 10623 Berlin, Germany

Supporting Information

ABSTRACT: The influence of poly(vinyl alcohol) (PVA) in the synthesis of SBA-15 was investigated. It was found that, by the addition of PVA, the surface area and porosity of SBA-15 is increased, while the structure and size of the mesopores remain unchanged. Nitrogen sorption measurements indicate that PVA introduces additional pores with pore sizes of around 2 nm into the pore wall. Thus, a simple way of improving the porosity of mesoporous silica is presented that could enhance transport of substrates through the porous system, important for catalytic applications and also beneficial for replication and nanocasting purposes. We, furthermore, show that a heterogeneous catalyst, Pt/SBA-15, with high surface area can be prepared by the addition of PVA-stabilized platinum nanoparticle sols.

KEYWORDS: SBA-15, mesoporous silica, PVA, platinum, cyclooctadiene hydrogenation, heterogeneous catalysis

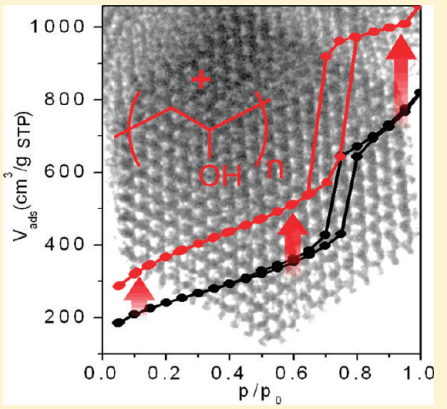

1. INTRODUCTION

The search for materials with high surface area and at the same time relatively large pore volumes and defined structures is still a challenging task for material scientists. High-surface-area materials are beneficial for any application requiring surface interactions with substrates, such as catalysis and sorption. However, materials with very high surface areas most often have small pore sizes,[1−3] which can hinder the diffusion of substrates and thus slow down catalytic conversions. On the other hand, enlargement of the pores most often yields decreasing surface areas. Several works[4,5] have, for example, reported that the pore size of mesoporous silicas can be enlarged using micelle expanders; however, this was achieved at the expense of the overall surface area. One interesting exception has been reported, that is, the addition of phosphoric acid to the preparation protocol of SBA-15, which increases the surface area and mesopore volume.[6,7] Another pathway to increase the overall pore volume and surface area without decreasing the mesopore size is the introduction of a hierarchical porosity, that is, the formation of larger pores connected by smaller ones. In several mesoporous silicas, such a structure is formed by the existence of micropores in the pore walls, connecting the often periodically arranged mesopores.[8−11] These micropores are crucially important for the use of ordered mesoporous silicas as a hard template for the generation of mesoporous carbon and other materials because these bridges between the mesopores allow the generation of stable mesoporous replicas.[12] Consequently, several approaches have been used to tailor the amount and size of the micro- and mesopores, and it has been reported that hierarchical porosity can be obtained by approaches such as postsynthesis acidic or basic treatments.[13−15] Another attempt to achieve hierarchical, bimodal pore-size distributions in mesoporous silica is to use templates of different sizes that do not interfere with each other. This is rather simple when using rigid latex templates,[16,17] which are, however, restricted toward smaller pore sizes to about 30−50 nm but are more demanding for soft, self-organizing systems, like micelles and lytropic phases formed from surfactants. These molecules usually form mixed aggregates, yielding the formation of just one pore size, often reflecting the average value of the two surfactants alone.[18] Fluorinated surfactants have been applied as additional templates together with amphiphilic block copolymers because they cannot form mixed micelles with these hydrocarbons. Indeed, mesoporous silicas with bimodal porosity can be prepared using this approach.[19] Also, dendritic polymers together with block-copolymer micelles have been used to prepare hierarchical, bimodal porous silicas.[20]

In this study, we report another method that can improve the mesopore connectivity and thus enhance the surface area and pore volume of the silicas without decreasing the mesopore diameter by the addition of low amounts of poly(vinyl alcohol) (PVA) to the reaction mixture. Ordered mesoporous silica SBA-15[21] was chosen as the reference material for this investigation. SBA-15 is prepared using the triblock copolymer P123 as the template, yielding a two-dimensional hexagonal arrangement of cylindrical pores. In recent years, this material was used for

Received: October 4, 2010
Revised: March 18, 2011
Published: March 31, 2011

various applications, e.g., in catalysis[22,23] purification[24,25] and as a hard template for the generation of other mesoporous materials.[26−31] The addition of small amounts of PVA to an otherwise unchanged preparation protocol seems to result in the introduction of an extra porosity connecting the cyclindrical mesopores without changing the mesopore size and structure of the SBA-15 material.

2. EXPERIMENTAL SECTION

Synthesis of SBA-15-V. A total of 0.5 g of P123 ($EO_{20}PO_{70}EO_{20}$, M_{av} = 5800) was dissolved in a mixture of distilled water (7.5 g) and a 2 M hydrochloric acid solution (15 g) with continuous stirring, and the temperature was controlled at ∼35 °C; after P123 was fully dissolved, a freshly prepared 1 wt % aqueous poly(vinyl alcohol) (PVA; M_{av} = 130 000) solution was added in different amounts. To this solution was added 1.05 g of tetraethoxysilane, and the resulting mixture was kept at ∼35 °C for 24 h, subsequently poured into a Teflon-lined autoclave, and aged at 80−150 °C for another 24 h. Finally, the sample was filtered, dried at 100 °C overnight, and calcined at 500 °C for 4 h. The samples show thermal and long-term stability under ambient conditions comparable to those observed for pure SBA-15 materials.

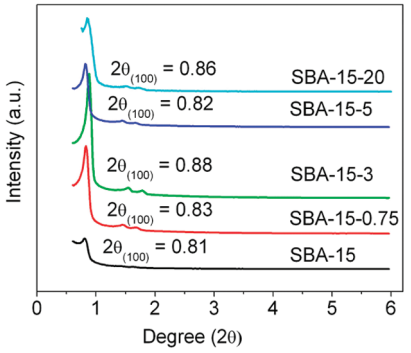

Figure 1. XRD patterns of SBA-15 synthesized with different amounts of PVA. The aging temperature for all of the samples was 100 °C.

Synthesis of Pt-SBA-15-3. The platinum sol was prepared by mixing 11 mL of a 0.0015 M H_2PtCl_6 solution with 3 mL of a 1.0 wt % PVA solution. Subsequently, 0.1 M $NaBH_4$ aqueous solutions were added dropwise, and stirring was continued for 5 min. The thus-obtained platinum sol (containing PVA and $NaBH_4$) was used to prepare the Pt-SBA-15-3 catalyst. The loading of platinum measured by inductively coupled plasma (ICP) analysis was 0.29 wt %.

Characterizations. X-ray diffraction (XRD) patterns were measured on a Bruker D8 Advance X-ray diffractometer using Cu $K\alpha_1$ irradiation. Transmission electron microscopy (TEM) images were obtained on a Philips CM12 instrument (120 keV), using carbon-coated copper grids (the specimens were loaded directly onto the copper grids; no solvent dispersion was used). Nitrogen sorption isotherms were determined at liquid-nitrogen temperature (−196 °C) with an Autosorb-1 apparatus. The sample was degassed at 150 °C overnight before measurement. The Brunauer−Emmett−Teller (BET) surface area was calculated by multiple-point (five-point) measurement in the relative pressure range of 0.05−0.30. The amount of metal in the samples was determined using a Perkin-Elmer 3300DV ICP. Thermogravimetric analysis measurements were carried out on a STA6000 from Perkin-Elmer.

Catalytic Tests. Catalytic reactions were carried out in a 100-mL five-necked flask with a water jacket in 80 mL of heptane at 60 °C under hydrogen pressure (1.1 bar). A total of 2.165 g (0.02 mol) of 1,

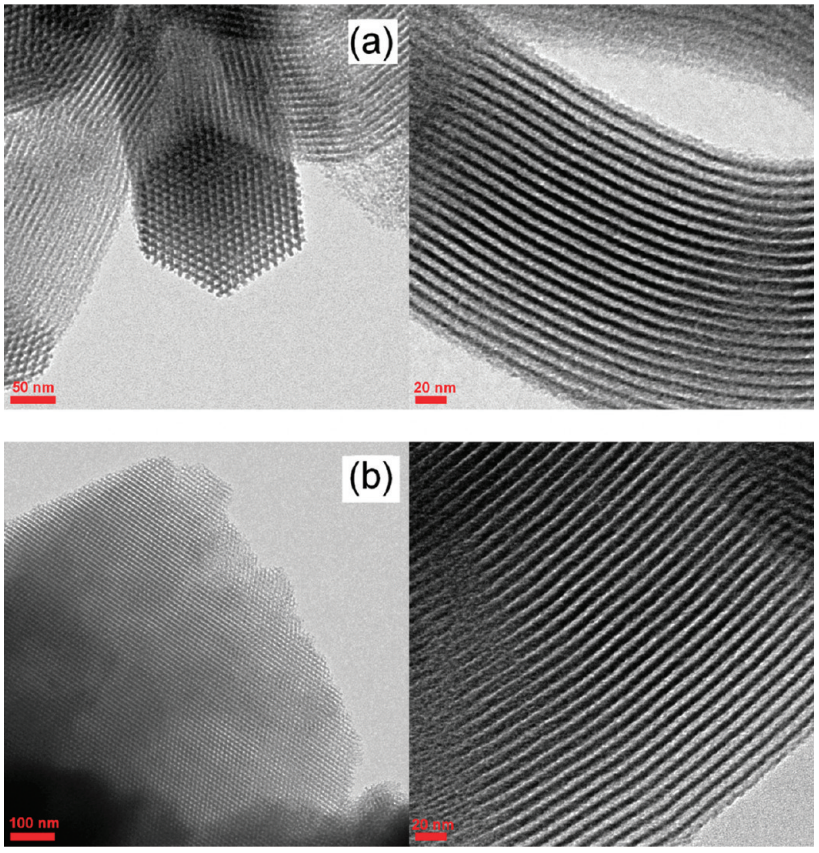

Figure 2. TEM images of SBA-15 synthesized under different conditions: (a) SBA-15; (b) SBA-15-3.

dx.doi.org/10.1021/cm1028639 |*Chem. Mater.* 2011, 23, 2062–2067

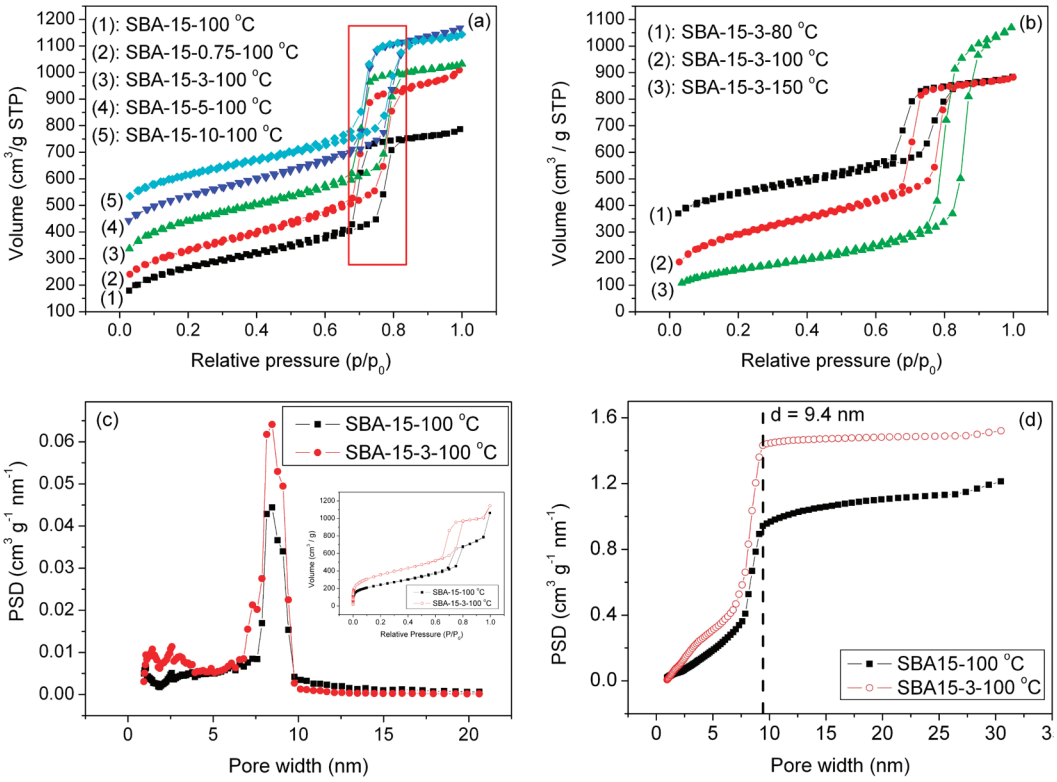

Figure 3. (a and b) Nitrogen sorption isotherms for SBA-15-100 °C synthesized with different PVA contents and aging temperatures. (c) Pore-size distribution derived from the nitrogen adsorption isotherms with micropore analysis (inset). (d) Cumulative pore volume for SBA-15 and SBA-15-3-100 °C (both obtained using the NLDFT method).

Table 1. Textural Properties of SBA-15 Synthesized under Different Conditions

sample	SA ($m^2\ g^{-1}$)[a]	Pa (nm)[b]	PV ($cm^3\ g^{-1}$)[c]
SBA-15-100 °C	877	9.7	1.15
SBA-15-0.75-100 °C	986	9.7	1.48
SBA-15-3-100 °C	1177	9.7	1.43
SBA-15-5-100 °C	1124	9.7	1.58
SBA-15-10-100 °C	1182	9.7	1.49
SBA-15-3-80 °C	1248	8.7	1.41
SBA-15-3-150 °C	555	14.8	1.64

[a] SA = surface area calculated by the BET method. [b] Pa = pore size calculated from the adsorption branch. [c] PV = pore volume calculated at $p/p_0 = 0.99$.

5-cyclooctadiene (COD) and 1.08 mg of a metal catalyst were used for each catalytic test. Samples were taken out periodically and analyzed by gas chromatography.

3. RESULTS AND DISCUSSION

The pure SBA-15 was synthesized using a procedure similar to that reported elsewhere.[21] To the reaction mixtures was added in different amounts a freshly prepared 1 wt % aqueous PVA (M_{av} = 130 000) solution. Depending on the amount of PVA added, the samples were named SBA-15-V ("V" is the volume of the added PVA solution). Also, referring to the aging temperature, the samples were named as SBA-15-V-T. For example, "SBA-15-3-100 °C" means that SBA-15 was synthesized with 3 mL of 1 wt % PVA and aged at 100 °C for 24 h. To observe the porous silica, calcination at 500 °C for 4 h was carried out, sufficient to completely remove the organic phases (Figure S1 in the Supporting Information, SI).

Figure 1a shows the XRD patterns of the samples synthesized with different amounts of PVA. All patterns show an intensive peak at $2\theta = 0.8-0.9$ that corresponds to the (100) diffraction of the two-dimensional hexagonal structure of SBA-15, indicating the presence of an ordered pore structure and d_{100} values of 10.0−10.9 nm. The well-resolved (110) and (200) diffraction peaks indicate that there was no substantial change in the pore structure of the samples after PVA was added. For SBA-15-3 aged at different temperatures, the sample aged at 100 °C showed the highest 2θ value (Figure S2 in the SI).

The ordered pore structure of the samples was further proven by TEM measurements, as shown in Figures 2 and S3 in the SI. The samples possess well-ordered hexagonal arrays of mesopores, whether PVA is added or not. Thus, it can be stated that the addition of PVA does not influence or even deteriorate the order of the pluronic−silica composite.

Figure 3a shows the nitrogen sorption isotherms of the samples synthesized with different amounts of PVA. The corresponding porous characteristics are listed in Table 1. All samples show a defined step with a hysteresis loop corresponding to the filling of mesopores with narrow pore-size distributions. The nitrogen sorption isotherms show an increase of the surface area from 877 $m^2\ g^{-1}$ and a total pore volume from 1.15 $cm^3\ g^{-1}$ for SBA-15 to 1177 $m^2\ g^{-1}$ and 1.43 $cm^3\ g^{-1}$ for SBA-15-3. However, despite the increase in the surface area (∼34%) and porosity (∼24%), the pore size of the mesopores generated from the block copolymer is almost unchanged based on the

dx.doi.org/10.1021/cm1028639 |Chem. Mater. 2011, 23, 2062–2067

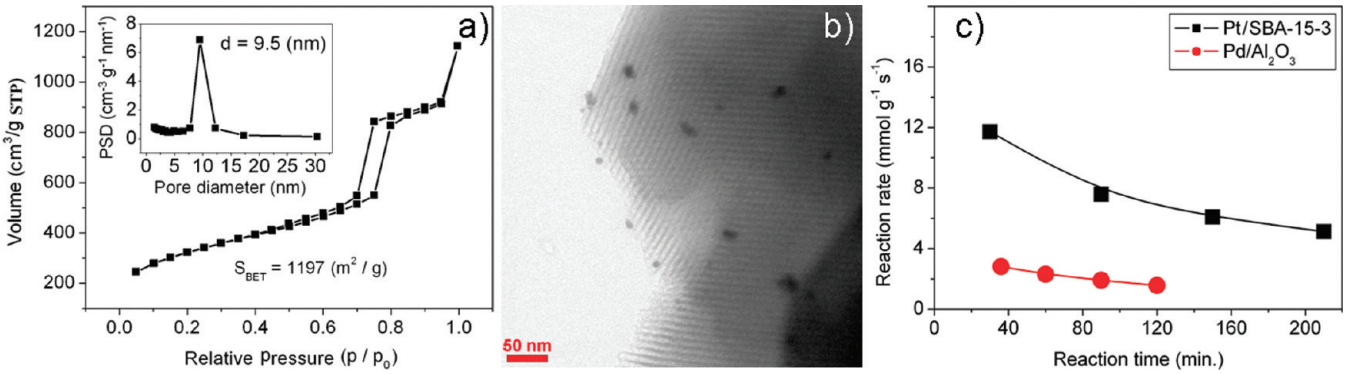

Figure 4. (a) Nitrogen sorption isotherms and pore-size distribution of Pt-SBA-15-3. (b) TEM images of Pt-SBA-15-3. (c) Reaction rate of Pt-SBA-15-3 and commercial Pd/Al_2O_3 for a COD hydrogenation reaction. (Note that the reaction rate was calculated based on the amount of noble metal; the reaction rate based on the overall amount of catalyst can be found in Figure S8 in the SI.)

Barrett−Joyner−Halenda (BJH) method on the adsorption branch (Figure S4 in the SI). A further increase of the PVA content does not yield further significant enhancement of the surface area or the pore volume.

It can be concluded that the addition of PVA does not influence the mesopores created by P123 and thus that the increase of the surface area and porosity is likely due to the creation of additional pores with smaller diameter in the materials. To prove this, nitrogen sorption isotherms for SBA-15-100 °C and SBA-15-3-100 °C with additional micropore analysis were carried out. Analysis of the pore-size distribution and the cumulative pore volume (obtained from nonlocal density functional theory, NLDFT) shown in Figures 3c,d and S5 in the SI indicates that there are indeed new, smaller pores created in SBA-15-3-100 °C.

The higher surface area and pore volume after the addition of PVA could be attributed to an additional porosity, introduced by PVA. This, however, would imply that the micelles formed from P123 do not deeply interact with PVA. It can be easily imagined that PVA does not interpenetrate the more hydrophobic PPO block in the micellar core, which would influence the micelle size and shape, reflected in a, not observed, change in the mesopore size and structure of the resulting silica. However, the PEO blocks forming the corona of the micelle and PVA are both hydrophilic and water-soluble and thus might be miscible in aqueous solutions. However, it has been shown that aqueous blends of PEO and PVA are immiscible and just show small interactions between the polymers[32] and that PVA/PEO cast films from aqueous blends show phase separation.[33] Thus, it can be assumed that the interaction of PVA and PEO is marginal and just occurs in the outer region of the PEO corona, the phase that is dispersed in the solvent and thus causes the microporosity.[34] Whether the additional mesopore connectivities are formed by single PVA chains or aggregated chains of PVA and PEO can, however, not be conclusively answered.

Also, the effect of the aging temperature on the structural properties of SBA-15-3 was investigated, and the results are shown in Figure 3b and Table 1. As expected, the surface area decreases and the pore size increases with increasing temperature, which might be due to aggregation of the PEO chains, as was suggested by Galarneau et al.[35] However, this trend is just observed up to a temperature of 80 °C, while further lowering of the temperature (e.g., 60 °C) yields materials with lowered surface area (Figure S6 in the SI). This effect was also observed for pure SBA-15 prepared at this temperature and was ascribed to a lower amount of mesopore connectivities due to hydration of the PEO chains.[35] It should be, however, also noted that for SBA-15 prepared at lower hydrothermal temperatures decreasing surface areas have also been observed to be influenced by the calcination temperature.[36]

PVA has been frequently used to stabilize catalytically active noble-metal particles in solutions and to further immobilize them on preformed solid supports to prepare heterogeneous catalysts.[37−44] It can, therefore, be envisaged that the approach shown here can be used for the synthesis of supported noble-metal catalysts by using PVA as, first, a stabilizer for the metal sol and as, second, an additional template in the synthesis of high-surface-area SBA-15. Platinum nanoparticles (Pt-NPs) supported on SBA-15 have been frequently described as good catalysts for, e.g., hydrogenation reactions.[45−47] Here a metal sol was prepared by the reduction of H_2PtCl_6 in the presence of 3 mL of a 1 wt % PVA solution. The resulting metal sol was added to the preparation of SBA-15 instead of the pure PVA solutions, yielding a material named Pt-SBA-15-3. A metal loading of 0.29 wt %, determined by ICP, was achieved using this protocol. The nitrogen sorption isotherms in Figure 4a show that the surface area of Pt-SBA-15-3 reaches 1197 $m^2\ g^{-1}$, thus again no decreases compared the sample prepared from pure PVA (SBA-15-3: 1177 $m^2\ g^{-1}$). This is different from other works,[48−50] where the surface area of SBA-15 decreases significantly after the loading of platinum. Also, no change in the pore size was observed before and after the loading of platinum. The TEM image of Pt-SBA-15-3 in Figure 4b shows that the Pt-NPs are homogeneously dispersed in the sample, with a mean particle size of ∼9 nm. Higher-magnification images indicate that at least some of the Pt-NPs are located within the mesopores of the samples (Figure S7 in the SI).

The catalytic activity of Pt-SBA-15-3 as a hydrogenation catalyst was tested using COD as the reactant and a hydrogen pressure of 1.1 bar. Figure 4c shows the reaction rate of Pt-SBA-15-3 and a commercial catalyst (Pd-NPs supported on Al_2O_3) in the hydrogenation of COD. As expected, the reaction rate decreases for both catalysts, with a similar decreasing trend. The rate of Pt-SBA-15-3 reaches 11.72 mmol $g^{-1}\ s^{-1}$ after 30 min of reaction and still with a value of 5.13 mmol $g^{-1}\ s^{-1}$ after 210 min, which is already 2 times the rate from Pd/Al_2O_3 since the beginning of the reaction. The catalyst can be, furthermore, recycled at least 4 times without an observable loss in activity.

dx.doi.org/10.1021/cm1028639 |*Chem. Mater.* 2011, 23, 2062–2067

4. CONCLUSION

In summary, a method improving the porosity of mesoporous silicas is reported. The addition of small amounts of PVA to the reaction mixture of, e.g., the synthesis of the ordered mesoporous silica, SBA-15, increases the surface area from 877 $m^2 g^{-1}$ (pure SBA-15) up to 1177 $m^2 g^{-1}$, without a significant change of the mesopore size or architecture. This can be explained by the formation of additional pores, formed from the PVA template, connecting the larger mesopores formed from the P123 template. For practical applications, such an increase in the surface area and additional porosity should facilitate interaction with the adsorbates and provide better transport channels through the material. Such properties are beneficial for their use as sorbents or catalyst supports. Still, it should be noted that the additional mesopore connectivities have small pore diameters; that is, these advantages will hold true just for smaller molecules. The enhanced mesopore connectivity should also make the silicas highly suitable templates for the generation of other mesoporous materials, like mesoporous carbons, metal oxides, or metals, by hard templating or nanocasting approaches. It can be envisaged that the mechanism proposed here generally holds for the synthesis of mesoporous silicas using PEO-based surfactants as templates. Thus, also additional mesopore connections should be formed in mesoporous silicas other than those with two-dimensional hexagonal porosity. Respective studies are currently being carried out in our group. The additional template, PVA, can further be used to stabilize metal nanoparticles. Thus, the synthesis of SBA-15 supported Pt-NP catalysts can be carried out in one step, by adding a PVA-stabilized metal sol to the common SBA-15 synthesis. Indeed, the surface area of this catalyst is well improved compared to that of pure SBA-15, while the mesostructure and pore size remained unchanged. As a consequence, a versatile one-pot approach to high-surface-area supported catalysts with enhanced transportation pathways could be achieved.

■ ASSOCIATED CONTENT

Supporting Information. Detailed synthetic procedure, BJH and NLDFT pore size distributions, additional TEM micrographs of samples SBA-15-0.75, SBA-15-5, SBA-15-3-80, and SBA-15-3-150, and catalytic results for cyclooctadiene hydrogenation based on the overall catalyst mass. This material is available free of charge via the Internet at http://pubs.acs.org.

■ AUTHOR INFORMATION

Corresponding Author

*E-mail: ciaczjj@gmail.com (J.Z.), arne.thomas@tu-berlin.de (A.T.).

■ ACKNOWLEDGMENT

Financial support from the Cluster of Excellence "Unifying Concepts in Catalysis" (supported by the Deutsche Forschungsgemeinschaft and hosted by the TU Berlin) is gratefully acknowledged.

■ REFERENCES

(1) Pujari, A. A.; Chadbourne, J. J.; Ward, A. J.; Costanzo, L.; Masters, A. F.; Maschmeyer, T. *New J. Chem.* **2009**, *33*, 1997.
(2) Wang, H. T.; Wang, Z. B.; Huang, L. M.; Mitra, A.; Holmberg, B.; Yan, Y. S. *J. Mater. Chem.* **2001**, *11*, 2307.
(3) Park, K. H.; Sung, I. K.; Kim, D. P. *J. Mater. Chem.* **2004**, *14*, 3436.
(4) Cao, L. A.; Man, T.; Kruk, M. *Chem. Mater.* **2009**, *21*, 1144.
(5) Fan, J.; Yu, C. Z.; Wang, L. M.; Tu, B.; Zhao, D. Y.; Sakamoto, Y.; Terasaki, O. *J. Am. Chem. Soc.* **2001**, *123*, 12113.
(6) Colilla, M.; Balas, F.; Manzano, M.; Vallet-Regi, M. *Chem. Mater.* **2007**, *19*, 3099.
(7) Colilla, M.; Balas, F.; Manzano, M.; Vallet-Regi, M. *Solid State Sci.* **2008**, *10*, 408.
(8) Goltner, C. G.; Smarsly, B.; Berton, B.; Antonietti, M. *Chem. Mater.* **2001**, *13*, 1617.
(9) Silvestre-Albero, A.; Jardim, E. O.; Bruijn, E.; Meynen, V.; Cool, P.; Sepulveda-Escribano, A.; Silvestre-Albero, J.; Rodriguez-Reinoso, F. *Langmuir* **2009**, *25*, 939.
(10) Ryoo, R.; Ko, C. H.; Kruk, M.; Antochshuk, V.; Jaroniec, M. *J. Phys. Chem. B* **2000**, *104*, 11465.
(11) Thomas, A.; Schlaad, H.; Smarsly, B.; Antonietti, M. *Langmuir* **2003**, *19*, 4455.
(12) Joo, S. H.; Ryoo, R.; Kruk, M.; Jaroniec, M. *J. Phys. Chem. B* **2002**, *106*, 4640.
(13) Escax, V.; Delahaye, E.; Imperor-Clerc, M.; Beaunier, P.; Appay, M. D.; Davidson, A. *Microporous Mesoporous Mater.* **2007**, *102*, 234.
(14) Galarneau, A.; Cambon, H.; Di Renzo, F.; Fajula, F. *Langmuir* **2001**, *17*, 8328.
(15) Khodakov, A. Y.; Zholobenko, V. L.; Bechara, R.; Durand, D. *Microporous Mesoporous Mater.* **2005**, *79*, 29.
(16) Antonietti, M.; Berton, B.; Goltner, C.; Hentze, H. P. *Adv. Mater.* **1998**, *10*, 154.
(17) Zhou, Y.; Yu, S. H.; Thomas, A.; Han, B. H. *Chem. Commun.* **2003**, 262.
(18) Thomas, A.; Polarz, S.; Antonietti, M. *J. Phys. Chem. B* **2003**, *107*, 5081.
(19) Xing, R.; Lehmler, H. J.; Knutson, B. L.; Rankin, S. E. *Langmuir* **2009**, *25*, 6486.
(20) Nowag, S.; Wang, X. S.; Keilitz, J.; Thomas, A.; Haag, R. *ChemCatChem* **2010**, *2*, 807–811.
(21) Zhao, D. Y.; Feng, J. L.; Huo, Q. S.; Melosh, N.; Fredrickson, G. H.; Chmelka, B. F.; Stucky, G. D. *Science* **1998**, *279*, 548.
(22) Chmielarz, L.; Kustrowski, P.; Dziembaj, R.; Cool, P.; Vansant, E. F. *Microporous Mesoporous Mater.* **2010**, *127*, 133.
(23) Srivastava, R.; Srinivas, D.; Ratnasamy, P. *J. Catal.* **2005**, *233*, 1.
(24) Lee, J. W.; Tra, P. T.; Kim, S. I.; Roh, S. H. *J. Nanosci. Nanotechnol.* **2008**, *8*, 5152.
(25) Jun, Y. S.; Huh, Y. S.; Park, H. S.; Thomas, A.; Jeon, S. J.; Lee, E. Z.; Won, H. J.; Hong, W. H.; Lee, S. Y.; Hong, Y. K. *J. Phys. Chem. C* **2007**, *111*, 13076.
(26) Titirici, M. M.; Thomas, A.; Antonietti, M. *J. Mater. Chem.* **2007**, *17*, 3412.
(27) Thomas, A.; Goettmann, F.; Antonietti, M. *Chem. Mater.* **2008**, *20*, 738.
(28) Jun, Y. S.; Hong, W. H.; Antonietti, M.; Thomas, A. *Adv. Mater.* **2009**, *21*, 4270.
(29) Tiemann, M. *Chem. Mater.* **2008**, *20*, 961.
(30) Yang, H. F.; Zhao, D. Y. *J. Mater. Chem.* **2005**, *15*, 1217.
(31) Lu, A. H.; Schuth, F. *Adv. Mater.* **2006**, *18*, 1793.
(32) Paladhi, R.; Singh, R. P. *J. Appl. Polym. Sci.* **1994**, *51*, 1559.
(33) Abd Alla, S. G. *J. Appl. Polym. Sci.* **2004**, *94*, 167.
(34) Smarsly, B.; Polarz, S.; Antonietti, M. *J. Phys. Chem. B* **2001**, *105*, 10473.
(35) Galarneau, A.; Cambon, N.; Di Renzo, F.; Ryoo, R.; Choi, M.; Fajula, F. *New J. Chem.* **2003**, *27*, 73.
(36) Yoon, S. B.; Kim, J. Y.; Kooli, F.; Leec, C. W.; Yu, J. S. *Chem. Commun.* **2003**, 1740.
(37) Chan-Thaw, C. E.; Villa, A.; Katekomol, P.; Su, D. S.; Thomas, A.; Prati, L. *Nano Lett.* **2010**, *10*, 537.
(38) Villa, A.; Wang, D.; Su, D. S.; Prati, L. *ChemCatChem* **2009**, *1*, 510.
(39) Chan-Thaw, C. E.; Villa, A.; Prati, L.; Thomas, A. *Chem.—Eur. J.* **2011**, *17*, 1052.
(40) Roy, P. S.; Bagchi, J.; Bhattacharya, S. K. *Transition Met. Chem.* **2009**, *34*, 447.

(41) Siani, A.; Wigal, K. R.; Alexeev, O. S.; Amiridis, M. D. *J. Catal.* **2008**, *257*, 16.
(42) Harada, M.; Einaga, H. *Catal. Commun.* **2004**, *5*, 63.
(43) Porta, F.; Prati, L.; Rossi, M.; Scari, G. *J. Catal.* **2002**, *211*, 464.
(44) Porta, F.; Prati, L.; Rossi, M.; Coluccia, S.; Martra, G. *Catal. Today* **2000**, *61*, 165.
(45) Song, H.; Rioux, R. M.; Hoefelmeyer, J. D.; Komor, R.; Niesz, K.; Grass, M.; Yang, P. D.; Somorjai, G. A. *J. Am. Chem. Soc.* **2006**, *128*, 3027.
(46) Huang, W.; Kuhn, J. N.; Tsung, C. K.; Zhang, Y.; Habas, S. E.; Yang, P.; Somorjai, G. A. *Nano Lett.* **2008**, *8*, 2027.
(47) Rioux, R. M.; Komor, R.; Song, H.; Hoefelmeyer, J. D.; Grass, M.; Niesz, K.; Yang, P. D.; Somorjai, G. A. *J. Catal.* **2008**, *254*, 1.
(48) Chytil, S.; Glomm, W. R.; Blekkan, E. A. *Catal. Today* **2009**, *147*, 217.
(49) Kumar, M. S.; Chen, D.; Holmen, A.; Walmsley, J. C. *Catal. Today* **2009**, *142*, 17.
(50) Jiao, L.; Regalbuto, J. R. *J. Catal.* **2008**, *260*, 342.